Original Paper Environ. Control Biol., **45** (1), 39–46, 2007

Chlorophyll Fluorescence Imaging at 77 K for Assessing the Heterogeneously Distributed Light Stress Over a Leaf Surface

Kotaro TAKAYAMA, Yoshiaki SAKAI, Hiroshige NISHINA and Kenji OMASA*

Faculty of Agriculture, Ehime University, 3–5–7 Tarumi, Matsuyama, Ehime 790–8566, Japan
Graduate School of Agricultural and Life Science, The University of Tokyo, 1–1–1 Yayoi, Bunkyo-ku, Tokyo 113–8657, Japan

(Received December 20, 2006)

We developed a chlorophyll fluorescence imaging system that is capable of capturing chlorophyll fluorescence intensity images (F683 and F730) of plant leaves at liquid nitrogen temperature (77 K). F683 is mainly emitted from photosystem (PS) II and light harvesting complex (LHC) II and F730 is mainly emitted from PS I and LHC I, therefore the ratio image of F730 to F683 (i.e. F730/F683) indicates the relative changes in the status of the light energy utilization in the photosystems, e.g. state transition, and can be used to produce maps of relative levels of light stress over a leaf's surface. Using this system, we assessed the heterogeneously distributed light stresses over kidney bean leaf surfaces, caused by light irradiance and representative photosynthesis inhibitor (DCMU and DTT) infiltration treatments. As a result, F730/F683 increased in the light-irradiated leaf areas but remained at a lower value in the DCMU- and DTT-infiltrated leaf areas. These results prove that this 77 K chlorophyll fluorescence imaging system is capable of assessing the light stress that is heterogeneously distributed over a leaf surface.

Keywords : image diagnosis, photoinhibition, photosynthesis inhibitor, photosystem, state transition

INTRODUCTION

Chlorophyll fluorescence is emitted from chlorophyll *a* pigment and, therefore, chlorophyll fluorescence imaging techniques can be used for the early detection of invisible photosynthetic dysfunction of plant leaves, as pioneered by Omasa et al. (1987) and Daley et al. (1989). Furthermore, many useful chlorophyll fluorescence parameters, such as NPQ and Φ_{PSII}, which quantify photosynthetic activity, have been developed (Genty et al., 1989; Bilger and Björkman, 1990; Krause and Weis, 1991; Maxwell and Johnson, 2000) and applied to imaging techniques for assessing the heterogeneous distribution of photosynthetic activity over the plant leaf (Daley, 1995; Genty and Meyer, 1995; Rolfe and Scholes, 1995; Siebke and Weis, 1995; Lichtenthaler and Miehé, 1997; Omasa and Takayama, 2003).

NPQ, which is used to evaluate photosynthetic stresses caused by excessive light energy input, is one of the most useful chlorophyll fluorescence non-photochemical quenching parameters (Müller et al., 2001). NPQ is a relative indicator of the strength of the transthylakoidal pH gradient and the ability of chloroplasts to dissipate excess excitation energy as heat (Krause and Weis, 1991; Maxwell and Johnson, 2000). Therefore, NPQ images have been used to assess various stresses

Corresponding author : Kotaro Takayama, fax : +81–89–946–9916,
e-mail : takayama@agr.ehime-u.ac.jp

distributed over the leaf surface (Osmond et al., 1998; Osmond and Park, 2001; Omasa and Takayama, 2003). However, in order to obtain an NPQ image, it is necessary to first obtain a preliminary chlorophyll fluorescence image under dark conditions (Daley, 1995; Osmond et al., 1998; Omasa and Takayama, 2003), but this preliminary measurement is bothersome.

Most chlorophyll fluorescence parameters, including NPQ, are measured at room temperature. However, we can also obtain quantitative information on plant physiological status by measuring chlorophyll fluorescence at liquid nitrogen temperature (77 K). At room temperature, chlorophyll fluorescence in the red and far-red regions is emitted mainly by photosystem (PS) II, and the fluorescence emanating from PS I contributes little. However, PS I fluorescence in the far-red region (720–725 nm) significantly increases with a great emission from light harvesting complex (LHC) I peaking around 740 nm at low temperatures (Krause et al., 1983; Krause and Weis, 1991; Govindjee, 1995). At 77 K, fluorescence can be roughly classified into two emission bands, with peaks at around 680–695 nm and 720–740 nm. The former waveband emanates from PS II and LHC II and the latter from PS I and LHC I (Krause and Weis, 1991; Govindjee, 1995). Hence, the relationship between 680–695 nm and 720–740 nm fluorescence at 77 K, i.e. the ratio of 720–740 nm fluorescence intensity to 680–695 nm fluorescence intensity, has been used as an indicator of photoinhibition (Osmond, 1981; Powles and Björkman, 1982; Krause et al., 1983; Krause and Weis, 1991).

In this study, we developed a system that captures chlorophyll fluorescence images at 77 K. Using this system, we assessed the light stresses that were heterogeneously distributed over leaf surfaces caused by light irradiance and photosynthesis inhibitor infiltration treatments.

MATERIALS AND METHODS

Plant material

Kidney bean (*Phaseolus vulgaris* L. cv. 'Morocco') seeds were sown in pots (12 cm in diameter and 10 cm tall) and grown for 8 weeks in a greenhouse. The pots were filled with artificial soil (mixture of vermiculite and perlite, 1:1, v/v). Air temperature and relative humidity were 26.5ºC and 45% during the day and 20.0ºC and 55% at night. Plants were watered daily with a nutrient solution (1:1,000 dilution of HYPONex). Fully expanded mature attached or detached leaves were used for the measurements.

77 K chlorophyll fluorescence imaging system

Figure 1 shows a schematic diagram of the 77 K chlorophyll fluorescence imaging system. This system captures chlorophyll fluorescence images of the leaf surface at liquid nitrogen temperature (77 K). A plant leaf was horizontally fixed on the outside bottom surface of a transparent glass beaker (10 cm in diameter and 6 cm deep) and was kept submerged in liquid nitrogen by jacking up a metal container filled with liquid nitrogen as necessary. Then the leaf was illuminated by pulsed blue light, i.e. the measuring light, provided by high-luminescence blue light-emitting diodes (LEDs) to excite chlorophyll fluorescence. The radiation spectrum of the blue LEDs is shown in Fig. 2 (Fig. 2 also shows the transmittance spectra of the band-pass filters that are mentioned later). The duration and interval of the measuring light pulses were 2 ms and 16.6 ms, respectively. The light intensity at the leaf surface was 0.3 μmol m^{-2} s^{-1}, which induces fully reduction of Q_A, initial quinone electron acceptor in PS II, because reoxidation of Q cannot take place at 77 K (Powles and Björkman, 1982). Therefore, all fluorescence imaging was done at the F_m level in this system.

Chlorophyll fluorescence images were captured with a cooled charge-coupled device (CCD) video camera (C5985-02; Hamamatsu Photonics) equipped with two band-pass filters in front of the lens. Figure 2 shows the transmittance spectra of the band-pass filters. The 683-nm and 730-nm band-pass filters (Optical Coatings Japan) transmitted fluorescence with peak wavelengths of 683 nm and 730 nm, respectively. By changing the band-pass filters, two chlorophyll fluorescence

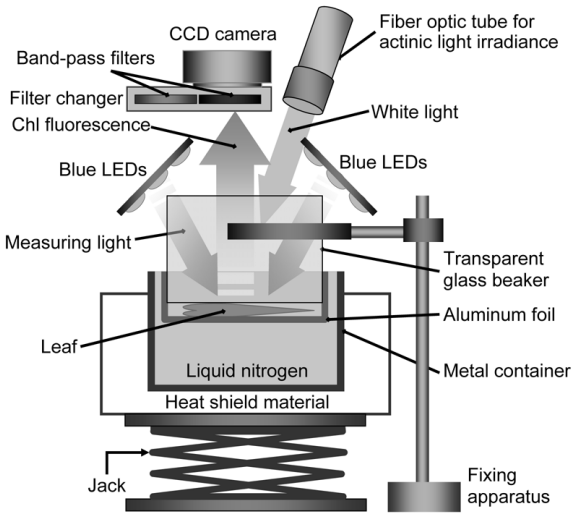

Fig. 1 Schematic diagram of the 77 K chlorophyll fluorescence imaging system. A leaf is kept submerged in liquid nitrogen by adjusting the jack level. The measuring light pulse from blue LEDs induces chlorophyll fluorescence. A filter changer, with 683-nm and 730-nm band-pass filters is placed in front of the lens of a CCD camera. White actinic light to irradiate the leaf surface is provided by four 180-W metal halide lamps via a fiber optic tube.

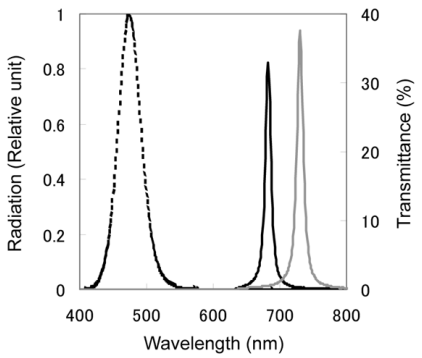

Fig. 2 Radiation spectrum of the blue LEDs used in the 77 K chlorophyll fluorescence imaging system (dotted line), and transmittance spectra of the 683-nm (black solid line) and 730-nm (gray solid line) band-pass filters.

images, F683 and F730, were captured for each leaf. F683 is mainly emitted from PS II and LHC II, and F730 is mainly emitted from PS I and LHC I but some of F730 was excited by the excitation energy transferred from PS II to PS I (Krause et al., 1983; Krause and Weis, 1991; Govindjee, 1995). Shutter speeds (exposure times) of the CCD camera were altered depending on the chlorophyll fluorescence intensities. The captured fluorescence images were recorded on a hard disk of a notebook computer at 720 horizontal×480 vertical pixels per frame with 8-bit resolution. Using the F683 and F730 images, the fluorescence ratio image of F730 to F683 (F730/F683), which indicates the changes in the light energy utilization status in the two photosystems (Krause et al., 1983; Krause and Weis, 1991), was calculated using software we produced ourselves.

EXPERIMENTAL TREATMENTS

Light irradiation treatment

Figure 3 shows a schematic diagram of the light irradiation treatment. An attached kidney bean leaf was fixed horizontally, and part of the leaf was covered with an opaque cover sheet (area A), a second part of the leaf was covered with an attenuation filter (area B), and a third part of the leaf was left uncovered (area C). Area A was exposed to dark conditions for 25 min, and areas B and C were irradiated with white actinic light at photosynthetic photon flux (PPF) densities of 250 and 1,000 μmol m^{-2} s^{-1}, respectively, for 5 min after 20 min dark-adaptation. The white actinic light was provided by four 180-W metal halide lamps (LS-M180; Sumita Optical Glass). Other environmental conditions were kept constant: air temperature was 20ºC, relative humidity was 50% and atmospheric O_2 and CO_2 concentrations were about 21% and 500 ppm, respectively. After the light irradiation treatment, the leaf was immediately immersed in liquid nitrogen and then chlorophyll fluorescence images (F683 and F730) were obtained. During the imaging procedure, the leaf was kept immersed in liquid nitrogen by adjusting the liquid nitrogen level as necessary.

DCMU infiltration treatment

The petiole of a detached kidney bean leaf was immersed in 10^{-6}-M 3-(3, 4-Dichlorophenyl)-1, 1-dimethylurea (DCMU), then the leaf was fixed horizontally in light at a PPF of 250 μmol m^{-2} s^{-1} for 5 h in order to induce the infiltration of DCMU. DCMU is an inhibitor of photosynthetic electron transport within PS II (Krause and Weis, 1991; Govindjee, 1995). After the DCMU infiltration treatment, the DCMU-infiltrated leaf was exposed to dark conditions for 20 min and then irradiated with actinic light at a PPF of 1,000 μmol m^{-2} s^{-1} for 5 min. After the brief light irradiation treatment, the leaf was immediately immersed in liquid nitrogen, and then F683 and F730 were measured.

DTT infiltration treatment

The petiole of a detached kidney bean leaf was immersed in 10-mM Dithiothreitol (DTT) and then the leaf was fixed horizontally in light at a PPF of 60 μmol m^{-2} s^{-1} for 6 h in order to induce the infiltration of DTT. DTT is an inhibitor of violaxanthin de-epoxidase, and prevents activation of the xanthophyll cycle that dissipates excessive light energy as heat when absorbed light energy is excessive (Krause and Weis, 1991; Osmond and Park, 2001). After the DTT infiltration treatment, the DTT-infiltrated leaf was exposed to dark conditions for 20 min, and then an F_m (maximum fluorescence intensity under dark conditions) image was obtained by using a saturation light pulse at a PPF of 1,800 μmol m^{-2} s^{-1} during the dark-adaptation. Next the leaf was irradiated with actinic light at a PPF of 300 μmol m^{-2} s^{-1} for 5 min in order to enhance heterogeneity over the leaf surface. At the end of the brief irradiation treatment, images of F (steady state fluorescence inten-

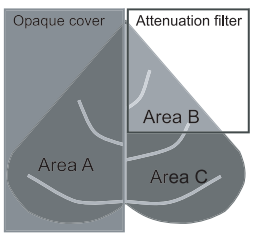

Fig. 3 Schematic diagram of the light irradiation treatment. Area A was covered with an opaque cover sheet and exposed to dark conditions for 25 min. Area B was covered with an attenuation filter. Area C was left uncovered. Areas B and C were irradiated with white actinic light at PPFs of 250 and 1,000 μmol m^{-2} s^{-1}, respectively, for 5 min after 20 min dark-adaptation.

sity under actinic light conditions) and F_m' (maximum fluorescence intensity under light conditions) were obtained. Using the fluorescence intensity images measured at room temperature, NPQ and Φ_{PSII} images were calculated using the following equations,

$$NPQ = \frac{F_m - F_m'}{F_m'} \qquad \Phi_{PSII} = \frac{F_m'/R_{SL} - F/R_{AL}}{F_m'/R_{SL}}$$

where R_{SL} and R_{AL} are the intensities of the saturation pulse and actinic light (Genty et al., 1989; Bilger and Björkman, 1990; Maxwell and Johnson, 2000; Müller et al., 2001). Immediately after the fluorescence imaging at room temperature, the leaf was immersed in liquid nitrogen and F683 and F730 were measured.

RESULTS AND DISCUSSION

Figure 4 shows visual, F683, F730 and F730/F683 images captured after the light irradiance treatment. No visible damage was observed over the leaf surface. However, fluorescence intensity significantly decreased in the light-treated areas (areas B and C) (see F683 and F730 in Fig. 4). The mean values of F683 within the regions denoted by the squares drawn in areas A, B and C in Fig. 4 were 154, 103 and 77, respectively; the mean values of F730 within the regions denoted by the squares in areas A, B and C were 129, 115 and 101, respectively. These results suggest that the light irradiance treatment lowered the chlorophyll fluorescence intensity regardless of its wavelength (Krause et al., 1983). Moreover, the reduction in F683 in the light-treated areas was larger than the reduction in F730. The substantial reduction in F683 seems to be due to strong non-photochemical quenching, mainly caused by the xanthophyll cycle (Krause et al., 1983; Krause and Weis, 1991). The mean values of F730/F683 within the regions denoted by the squares shown in areas A, B and C in Fig. 4 were 0.79, 1.08 and 1.27, respectively. This result shows that the light energy utilization status in the two photosystems altered in the light-treated areas, e.g. state transition (areas B and C) (Osmond, 1981; Powles and Björkman, 1982; Krause et al., 1983; Krause and Weis, 1991). Furthermore, the difference between values of F730/F683 in areas B and C was smaller than the difference in areas A and B. This result suggests that the status of light utilization status in the photosystems can be altered easily, even under low intensity light conditions (Müller et al., 2001; Mullineaux and Emlyn-Jones, 2004).

Figure 5 shows the visual, F683, F730 and F730/F683 images of a DCMU-infiltrated leaf after

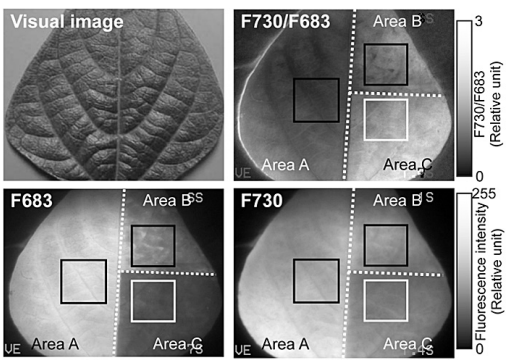

Fig. 4 Visual, F683, F730 and F730/F683 images after brief light irradiation treatment. Dotted lines separate areas A, B and C. The regions denoted by a square in each treated area were used for the calculation of mean values.

brief light irradiance treatment. In the F683 image, regions of high fluorescence were observed along veins. The same regions also had slightly higher fluorescence intensity in the F730 image. These results show that the regions along veins seem to have been infiltrated by DCMU, causing the photosynthetic electron transport in PS II to be severely inhibited and preventing a transthylakoidal pH gradient from forming (Krause and Weis, 1991; Govindjee, 1995; Osmond and Park, 2001). Consequently, non-photochemical processes, which are triggered by the transthylakoidal pH gradient, would not have been activated in those regions (Krause and Weis, 1991). As a result, F730/F683 in the DCMU-infiltrated regions was lower than that in the intervein regions. This result shows that the light energy utilization status in the photosystems did not change in the DCMU-infiltrated regions, because the xanthophyll cycle and the state-transition would not have been activated in those regions (Osmond, 1981; Powles and Björkman, 1982; Krause et al., 1983; Krause and Weis, 1991).

Figure 6 shows NPQ and Φ_{PSII} images of a DTT-infiltrated leaf after brief light irradiance treatment. A substantial reduction in NPQ was observed along veins. This result suggests that the DTT moves along veins and inhibits the activity of violaxanthin de-epoxidase (Müller et al., 2001). Thus the development of non-photochemical quenching would have been largely prevented in those regions (Osmond and Park, 2001). No significant decrease in Φ_{PSII}, however, was observed in the DTT-infiltrated regions. These results show that the inhibition of violaxanthin de-epoxidase by DTT does not have a significant impact on photosynthetic electron transport activity. Figure 7 shows F683, F730 and F730/F683 images of the same leaf as in Fig. 6. In the F683 image, fluo-

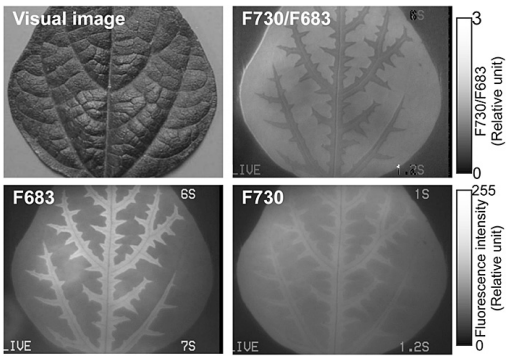

Fig. 5 Visual, F683, F730 and F730/F683 images of a DCMU-infiltrated leaf. The petiole of a detached leaf was immersed in 10^{-6}-M DCMU, under light at a PPF of 250 μmol m^{-2} s^{-1} for 5 h. After the DCMU infiltration treatment, the leaf was adapted to dark conditions for 20 min and then irradiated with white actinic light at a PPF of 1,000 μmol m^{-2} s^{-1} for 5 min.

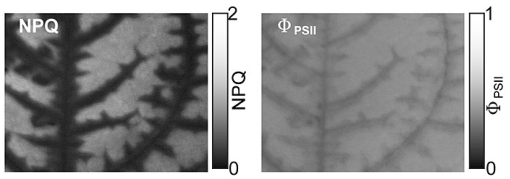

Fig. 6 NPQ and Φ_{PSII} images of a DTT-infiltrated leaf. The petiole of a detached leaf was immersed in 10-mM DTT for 6 h. The NPQ image was calculated from F_m and F_m' images. The F_m image was preliminarily measured under dark conditions, and the F_m' image was measured under actinic light conditions by supplying saturation pulse light at a PPF of 1,800 μmol m^{-2} s^{-1}. The Φ_{PSII} image was calculated from the F_m' and F images. The F image was measured under actinic light conditions at a PPF of 300 μmol m^{-2} s^{-1}.

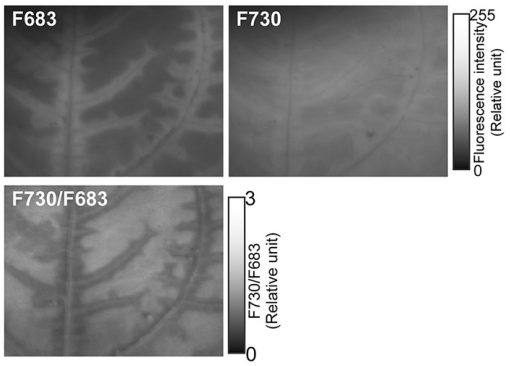

Fig. 7 F683, F730, F730/F683 images of a DTT-infiltrated leaf (the same leaf as shown in Fig. 6).

rescence quenching was observed only in the intervein regions, where DTT did not infiltrate; however, the DTT-infiltrated regions along the veins maintained higher fluorescence intensity. These observations show that non-photochemical quenching caused by the xanthophyll cycle is strictly prevented by DTT in the DTT-infiltrated regions. On the other hand, the effects of DTT infiltration could not be seen clearly in the F730 image. The value of F730/F683 increased in the intervein regions, although it remained at a lower level in the DTT-infiltrated regions. This result shows that the status of light energy utilization in the photosystems changed in the intervein regions, but did not change much in the DTT-infiltrated region (Osmond, 1981; Krause et al., 1983; Krause and Weis, 1991). Although DTT does inhibit violaxanthin de-epoxidase, it also reduces many components of photosynthetic apparatuses. So, the symptoms observed in the DTT-infiltrated region seem to be more or less affected by those concomitant effects.

At first glance, the F730/F683 image of the DCMU-infiltrated leaf seems similar to the F730/F683 image of the DTT-infiltrated leaf (see Figs. 5 and 7). However, quite different phenomena underpin these images. In the DTT-infiltrated regions, photosynthetic electron transport in PS II was not inhibited, and thus a transthylakoidal pH gradient was generated (Fig. 7), which was largely prevented in the DCMU-infiltrated regions (Fig. 5). Hence, it seems likely that there was some increase in F730/F683 in the DTT-infiltrated regions that was not detected in this experiment (Fig. 7).

In this study, we developed a 77 K chlorophyll fluorescence imaging system that is capable of capturing chlorophyll fluorescence images of plant leaves at liquid nitrogen temperature. We then used the imaging system to assess the light utilization status in the photosynthetic apparatus that is heterogeneously distributed over a leaf surface. Through three simple and easily-comprehensible experiments, we highlighted the merits of this system. First, this system quantitatively evaluates the light energy utilization status in the photosynthetic apparatus over a leaf surface without supplying saturation light pulses for the measurements. Moreover, this system does not require uniform distribution of measuring light within the measurement area because the effects of heterogeneous distribution of the measuring light are compensated for in the calculation of the fluorescence ratio image. Second, this system assesses photosynthetic photochemical activity without any preliminary measurements, for example the F_m measurement that is needed for NPQ measurement. These features enable analysis of the heterogeneous distribution of photosynthetic activity over a wider leaf area than would otherwise be possible.

REFERENCES

Bilger, W., Björkman, O. 1990. Role of the xanthophyll cycle in photoprotection elucidated by measurements of light-induced absorbance changes, fluorescence and photosynthesis in leaves of *Hedera canarienisis*. Photosyn. Res. **25**: 173–185.

Daley, P. F. 1995. Chlorophyll fluorescence analysis and imaging in plant stress and disease. Can. J. Plant Pathol. **17**: 167–173.

Daley, P. F., Raschke, K., Ball, J. T., Berry, J. A. 1989. Topography of photosynthetic activity of leaves obtained from video images of chlorophyll fluorescence. Plant Physiol. **90**: 1233–1238.

Genty, B., Briantais, J. M., Baker, N. R. 1989. The relationship between the quantum yield of photosynthetic electron transport and quenching of chlorophyll fluorescence. Biochim. Biophys. Acta **990**: 87–92.

Genty, B., Meyer, S. 1995. Quantitative mapping of leaf photosynthesis using chlorophyll fluorescence imaging. Aust. J. Plant Physiol. **22**: 277–284.

Govindjee. 1995. Sixty-three years since Kautsky: Chlorophyll *a* fluorescence. Aust. J. Plant Physiol. **22**: 131–160.

Krause, G. H., Briantais, J-M., Vernotte, C. 1983. Characterization of chlorophyll fluorescence quenching in chloroplasts by fluorescence spectroscopy at 77K. Biochim. Biophys. Acta **723**: 169–175.

Krause, G. H., Weis, E. 1991. Chlorophyll fluorescence and photosynthesis: the basics. Annu. Rev. Plant Physiol. Plant Mol. Biol. **42**: 313–349.

Lichtenthaler, H. K., Miehé, J. A. 1997. Fluorescence imaging as a diagnostic tool for plant stress. Trends Plant Sci. **2**: 316–320.

Maxwell, K., Johnson, G. N. 2000. Chlorophyll fluorescence: a practical guide. J. Exp. Bot. **51**: 659–668.

Müller, P., Li, X-P., Niyogi, K. K. 2001. Non-photochemical quenching. A response to excess light energy. Plant Physiol. **125**: 1558–1566.

Mullineaux, C. W., Emlyn-Jones, D. 2004. State transitions: an example of acclimation to low-light stress. J. Exp. Bot. **56**: 389–393.

Omasa, K., Shimazaki, K., Aiga, I., Larcher, W., Onoe, M. 1987. Image analysis of chlorophyll fluorescence transients for diagnosing the photosynthetic system of attached leaves. Plant Physiol. **84**: 748–752.

Omasa, K., Takayama, K. 2003. Simultaneous measurement of stomatal conductance, non-photochemical quenching, and photochemical yield of photosystem II in intact leaves by thermal and chlorophyll fluorescence imaging. Plant Cell Physiol. **44**: 1290–1300.

Osmond, C. B. 1981. Photorespiration and photoinhibition: some implications for the energetics of photosynthesis. Biochim. Biophys. Acta **639**: 77–98.

Osmond, C. B., Daley, P. F., Badger, M. R., Lüttge, U. 1998. Chlorophyll fluorescence quenching during photosynthetic induction in leaves of *Abutilon striatum* Dicks. infected with Abutilon mosaic virus, observed with a field-portable imaging system. Bot. Acta **111**: 390–397.

Osmond, C. B., Park, Y. M. 2001. Field-portable imaging system for measurement of chlorophyll fluorescence quenching. In "Air Pollution and Plant Biotechnology — Prospects for Phytomonitoring and Phytoremediation" (ed. by Omasa, K., Saji, H., Youssefian, S., Kondo, N.), Springer-Verlag, Tokyo, p 309–319.

Powles, S. B., Björkman, O. 1982. Photoinhibition of photosynthesis: effect on chlorophyll fluorescence at 77 K in intact leaves and in chloroplast membranes on *Nerium oleander*. Planta **156**: 97–107.

Rolfe, S. A., Scholes, J. D. 1995. Quantitative imaging of chlorophyll fluorescence. New Phytol. **131**: 69–79.

Siebke, K., Weis, E. 1995. Assimilation images of leaves of *Glechoma hederacea*: analysis of non-synchronous stomata related oscillations. Planta **196**: 155–165.